# Vibrational Analysis with the Symmetrically Combined Morse Potential Model for Antisymmetric Stretching in [ClDCl] Formed by Photodissociation of $(DCl)_2$

**Masaki Mitani,*,† Yasunori Yoshioka,*,† Dock-Chil Che,‡ and Toshio Kasai‡**

*Chemistry Department for Materials, Faculty of Engineering, Mie University, Kamihama, Tsu, Mie 514-8507, Japan, and Department of Chemistry, Graduate School of Science, Osaka University, Toyonaka, Osaka 560-0043, Japan*

*Received: October 31, 2003; In Final Form: March 6, 2004*

We estimate the line spacing between vibrational levels for the antisymmetric stretching in [ClDCl] to elucidate the origin of the oscillating structure on the translational energy distribution of the terminal D atom released by the photodissociation of $(DCl)_2$. The vibrational analysis with the symmetrically combined Morse potential model is performed for linear hydrogen-bonding [ClDCl] and the dependence of change in vibrational levels on the Cl−Cl distance is examined. It is found that the calculated assignment and observed spacing show good correspondence for $R_{ClCl} = 3.65$ or 3.70 Å, and it is therefore strongly suggested that the oscillation of dissociated D translational energy reflects the antisymmetric stretching vibration in the [ClDCl] counterpart.

## I. Introduction

One of the most important subjects in the study of reaction dynamics is probing the transition state in a chemical reaction because the nature of the potential energy surface in the near transition state determines the reaction dynamics and its branching ratios to exit channels.[1] Transient species of [XHX] are related to the transition state in the reaction of X + HX for hydrogen halide HX. By measuring the internal energy distribution of [XHX], one can extract direct information about the nature of interaction and the relevant potential energy surface of X + HX.[2,3]

In this context, the photoinitiated reaction of the weakly hydrogen-bonded dimer $(HX)_2$ has the potential to detect the [XHX] transient species by hydrogen elimination from $(HX)_2$. We have studied the [ClDCl] transient species by 243-nm photodissociation of $(DCl)_2$, which is nondestructively selected by using the electrostatic hexapole field.[4,5] The observed spectrum for translational energy distribution of the dissociated D atom revealed the oscillating structure, which is expected to be a footprint of the vibrational structure of [ClDCl]. The observed peaks of oscillating structure are tentatively assigned as 5010, 3490, 2680, 1890, and 1120 $cm^{-1}$, which have the spacing 1520, 810, 790, and 770 $cm^{-1}$.

Quantum chemical calculations at the various levels for $(HX)_2$ have been reported,[6−14] and it has been found that the global minimum of $(HCl)_2$ is a planar L-shaped geometry and the terminal H atom is almost orthogonal to the nearly linear ClHCl counterpart.[6,9−12] The intermolecular potential energy surface for the ground state of $(HCl)_2$ has also been examined extensively and a few analytical model potentials based on the theoretical calculations[6,10] or the experimental observations[15] have been proposed.

The electronic structure calculations including the electron correlations by spin-coupling-optimized generalized valence bond (SOGVB) and configuration interaction (CI) methods,[16] by second-order Møller−Plesset perturbation (MP2), multireference configuration interaction (MRCI), and multiconfiguration self-consistent field (MCSCF) methods[17] or by relativistic MP2 method[18] have been applied to linear and nonlinear [ClHCl]. The stationary points of Cl + HCl → ClH + Cl have been investigated, and the Cl−Cl distance at the linear stationary point of the transition state region has been predicted as 2.942−3.090 Å (ref 16), 2.940−2.984 Å (ref 17), and 2.962−2.963 Å (ref 18). The separations between Cl atoms are much shorter in the transition state of [ClHCl] (about 3.0 Å) than in the ground state of $(HCl)_2$ (about 3.8 Å). In ref 17, it has been reported that the bending potential on the [ClHCl] surface is rather flat and the changes in $R_{HCl}$ upon bending are in the range of 0.002−0.015 Å, suggesting a weak coupling of $R_{HCl}$ with the bending angle.

The photodetachment spectra of $[ClHCl]^-$ and $[ClDCl]^-$ have been simulated theoretically by using the semiempirical London−Eyring−Polanyi−Sato (LEPS) potential energy surface[3,19−22] or by using the ab initio MRCI potential energy surface.[23,24] In refs 3 and 23, the one-dimensional model has been used to investigate qualitatively the positions and intensities of peaks, and it has been mentioned that the motion along the antisymmetric vibration is a good approximation to the trajectory in the case of a heavy−light−heavy system such as [ClHCl]. The reason for the one-dimensional approach has been described in ref 3 clearly as follows. The antisymmetric vibration is nealy perpendicular to the minimum energy path, which leads to dissociation Cl + HCl via the reactant or product valleys. The antisymmetric stretch of the complex [ClHCl] is therefore poorly coupled to the reaction coordinate, and it should be able to explain the experimental peak positions and intensities with a one-dimensional model in which only the antisymmetric stretch of the complex is considered.

The LEPS potential and analytical potential which give the best fit to the experiment with $[ClHCl]^-$ and $[ClDCl]^-$ were

* Authors to whom correspondence should be addressed. M.M.: phone +81-59-231-9256; fax +81-59-231-9742; e-mail mitani@chem.mie-u.ac.jp. Y.Y.: phone +81-59-231-9742; fax +81-59-231-9742; e-mail yyoshi@chem.mie-u.ac.jp.

† Mie University.

‡ Osaka University.

10.1021/jp037302i CCC: $27.50 
Published on Web 05/25/2004

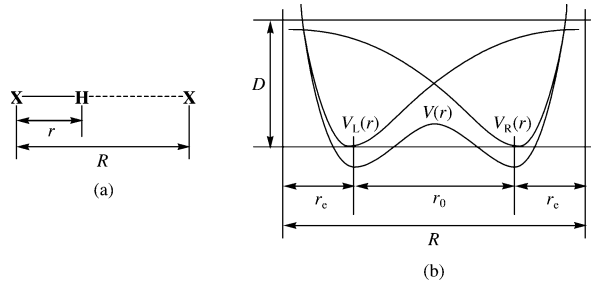


**Figure 1.** (a) Linear symmetric hydrogen bond and (b) symmetrically combined Morse potential.

compared in ref 3. Although the barrier is slightly higher in the experimental potential, the biggest difference is that the outer walls are too steep and the separation between the minima is too small in the LEPS potential. The simulated peak spacings from the LEPS surface therefore tend to be too large, and the simulated $v = 0$ peak is too intense.

The vibrational levels for the lowest $^2\Sigma$ and $^2\Pi$ states of [ClHCl] and [ClDCl] with linear structure obtained from the MRCI potential were reported in refs 23 and 24. The first energy gaps between the lowest two vibrational levels for $^2\Sigma$ and $^2\Pi$ states of [ClDCl] were shown respectively as about 2000 and 2500 $cm^{-1}$, where the calculated line positions were scaled by 0.75 to match the experimental values, indicating that the MRCI potential for antisymmetric stretching in [ClDCl] overestimates the spacing between vibrational levels. These energy separations by the MRCI calculation, even after scaling, are, however, larger by about 500 $cm^{-1}$ than our photodissociation spacing of about 1500 $cm^{-1}$ between the first and second peaks.

Further analysis of the potential energy curves and vibrational levels for antisymmetric stretching in [ClDCl] is therefore crucial to elucidate the origin of the experimentally detected oscillating spectrum with about 1500 or 800 $cm^{-1}$ for the first or higher spacing, respectively, in the $(DCl)_2$ photodissociation. In this work, the vibrational levels for the antisymmetric stretching mode $Q = (R_{ClD} - R_{DCl})/2^{1/2}$ in [ClDCl] are estimated by applying the symmetrically combined Morse potential model[25] to make a comparison with the experimental observation. The purpose of this study is to qualitatively confirm whether the experimental oscillating structure can be assigned as antisymmetric stretching vibrations in [ClDCl] or not. We perform the vibrational analysis for linear [ClDCl] under the Morse potential. The dependence of line spacing on the Cl−Cl distance is examined since the $R_{ClCl}$ is much different in the transition state of ClHCl and in the ground state of $(HCl)_2$, and the good correspondence between calculated and observed results is found within the one-dimensional model.

## II. The Symmetrically Combined Morse Potential Model for Vibrational Analysis

The symmetrical double-minimum potential constructed with the Morse potential was recently proposed to carry out the vibrational analysis of the one-dimensional hydrogen-bonding system (X−H···X) and it was demonstrated that analytical calculation of tunneling splitting with associated Laguerre functions works rather well.[25] In this model, the double-minimum potential $V(r)$ for [XHX] is obtained by combining the individual Morse potentials $V_L(r)$ for XH and $V_R(r)$ for HX (inverse of $V_L(r)$) as given in eqs 1−3 and as shown in Figure 1, parts a and b,

$$V(r) = V_L(r) + V_R(r) \tag{1}$$

$$V_L(r) = D[1 - \exp\{-\alpha(r - r_e)\}]^2 - D \tag{2}$$

$$V_R(r) = D[1 - \exp\{\alpha(r - r_0 - r_e)\}]^2 - D \tag{3}$$

where $D$ is the dissociation energy of XH, $r_e$ is the equilibrium distance X−H, $r_0$ is the distance between minima of $V_L(r)$ and $V_R(r)$, $R$ is the distance X−X, and $\alpha$ is related to the force constant of $V_L(r)$ and $V_R(r)$.

The Schrödinger equation for the whole [XHX] system (eqs 4 and 5) is variationally solved by expanding the wave function $\{\Psi\}$ under $V(r)$ (eq 6) as a linear combination of the eigenfunctions $\{\Phi^L\}$ for XH under $V_L(r)$ (eqs 7 and 8) and the eigenfunctions $\{\Phi^R\}$ for HX under $V_R(r)$ (eqs 9 and 10).

$$\hat{H}\Psi = E\Psi \tag{4}$$

$$\hat{H} = -\frac{\hbar^2}{2\mu}\frac{d^2}{dr^2} + V(r) \tag{5}$$

$$\Psi_v = \sum_{l=0}^{N} C_{lv}^{L}\,\Phi_l^L + \sum_{m=0}^{N} C_{mv}^{R}\,\Phi_m^R \tag{6}$$

$$\hat{H}_L = -\frac{\hbar^2}{2\mu}\frac{d^2}{dr^2} + V_L(r) \tag{7}$$

$$\hat{H}_L\Phi_v^L = E_v^L\,\Phi_v^L \tag{8}$$

$$\hat{H}_R = -\frac{\hbar^2}{2\mu}\frac{d^2}{dr^2} + V_R(r) \tag{9}$$

$$\hat{H}_R\Phi_v^R = E_v^R\,\Phi_v^R \tag{10}$$

where $\mu$ is the reduced mass of XH. The eigenvalue problem can result in solving the following secular equation,

$$\det|H_{ij} - ES_{ij}| = 0 \tag{11}$$

$$H_{ij} = \int \Phi_i \hat{H} \Phi_j\, dr \tag{12}$$

$$S_{ij} = \int \Phi_i \Phi_j\, dr \tag{13}$$

where $i$ and $j$ are the serial numbers of basis functions in eq 6. The eigenfunctions $\{\Phi^L\}$ and $\{\Phi^R\}$ are analytically given by adopting the associated Laguerre function, and therefore, the integrals included in matrix elements (eqs 12 and 13), which are needed in solving the secular equation for the whole system (eq 11), can be represented by gamma functions and Bessel functions. The analytical expressions of integrals are described in ref 25.

We investigate the vibrational levels in [ClDCl] produced by the photodissociation of $(DCl)_2$. The stable geometry of $(HCl)_2$ was predicted by first principle calculations, using various approximations, for example, MP2,[11,12] coupled-cluster (CCSD(T)),[12] and density functional (B3LYP),[26] as the L-shaped geometry with $C_s$ symmetry. It was reported that two HCl are located so as to be almost orthogonal with each other and the ClHCl moiety has a nearly linear structure. Figure 2 shows the optimized geometry of $(HCl)_2$ by using the B3LYP method.[26] Although small (BS1: Pople's 6-31G(d,p) for H and for Cl) and large (BS2: Huzinaga's (6s)/[3s] for H with one diffuse s function plus four polarization p and d functions and McLean and Chandler's (12s9p)/[6s5p] for Cl with two diffuse s and p functions plus four polarization d and f functions) basis sets

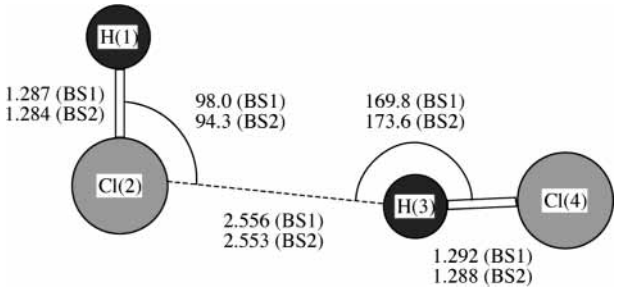


**Figure 2.** Optimized geometries of $(HCl)_2$ obtained by the B3LYP method. Two types of basis set were used: BS1, Pople's 6-31G(d,p) for H and for Cl; BS2, Huzinaga's (6s)/[3s] for H with one diffuse s plus four polarization p and d functions and McLean and Chandler's (12s9p)/[6s5p] for Cl with two diffuse s and p plus four polarization d and f functions.

**TABLE 1: Morse and Experimental Energy Separations between Vibrational Levels 0 and 5 for HCl and DCl[a]**

| | HCl | | DCl | |
|---|---|---|---|---|
| level | Morse | exptl[b] | Morse | exptl[b] |
| 0−1 | 2870 | 2886 | 2083 | 2091 |
| 1−2 | 2750 | 2782 | 2021 | 2037 |
| 2−3 | 2629 | 2679 | 1959 | 1984 |
| 3−4 | 2509 | 2576 | 1897 | 1931 |
| 4−5 | 2389 | 2473 | 1835 | 1878 |

[a] Vibrational energies are given in $cm^{-1}$. [b] Experimental energies are taken from refs 28 and 29.

were adopted in the optimization, the obtained structures were similar and the differences in optimized parameters were small. It was also suggested that the coupling between antisymmetric stretching and bending modes is weak in the transition region of [ClHCl].[3,17] Thus, we assumed that [ClDCl] has a linear atomic configuration and applied the symmetrically combined Morse potential model[25] to perform the vibrational analysis of antisymmetric stretching.

The parameters used in this study, which determine the Morse potential for HCl, are taken from ref 27, and the values of the parameters are as follows: $r_e = 1.275$ Å, $D = 106.3$ kcal/mol, and $\alpha = 1.86873$ $Å^{-1}$. These parameters give the energy separations between vibrational levels $v = 0-5$ listed in Table 1 together with experimental values[28,29] for HCl and DCl. The agreement between calculation and experiment is good although the separations of the former become smaller than experimental energy separations for higher vibrational levels as mentioned in ref 27.

Here, we note the convergence of the basis set number used in the calculation of vibrational analysis. The energy separations between vibrational levels $v = 0-4$ are converged respectively within 1 $cm^{-1}$ by applying the following number of eigenfunctions $\{\Phi^L\}$ and $\{\Phi^R\}$ to expand the wave function $\{\Psi\}$ ($N$ in eq 6): 11 for $R_{ClCl} = 3.50$ and 3.55 Å, 12 for $R_{ClCl} = 3.60$, 3.65, and 3.70 Å, and 13 for $R_{ClCl} = 3.75$, 3.80, and 3.85 Å. The number of obtained vibrational levels is twice the above basis set number, and these results are given below.

## III. Vibrational Levels for the Double-Minimum Morse Potential of [ClDCl]

We give the calculated results by using the symmetrically combined Morse potential in Table 2 and Figure 3a−d. Table 2 summarizes the energy separations between vibrational levels $v = 0-4$ of [ClDCl] at various Cl−Cl distances, and Figure 3a−d shows the vibrational energy levels of [ClDCl] for $R_{ClCl} = 3.50$, 3.60, 3.70, and 3.80 Å. The superscripts + and − for the vibrational level $v$ in Table 2 and Figure 3a−d indicate respectively the vibrational states represented by the wave function with plus and minus combinations of Morse eigenfunctions $\{\Phi^L\}$ and $\{\Phi^R\}$.

**TABLE 2: Potential Barriers between Double Minima and Energy Separations between Vibrational Levels 0 and 4 for [ClDCl] at Various Cl−Cl Distances[a]**

| | $R_{ClCl}$ (Å) [barrier] | | | | | | | |
|---|---|---|---|---|---|---|---|---|
| level | 3.50 [1161] | 3.55 [1706] | 3.60 [2326] | 3.65 [3008] | 3.70 [3739] | 3.75 [4504] | 3.80 [5313] | 3.85 [6140] |
| $0^+-0^-$ | 32 | 7 | 1 | 0 | 0 | 0 | 0 | 0 |
| $0^--1^+$ | 727 | 942 | 1153 | 1301 | 1402 | 1482 | 1548 | 1605 |
| $1^+-1^-$ | 384 | 200 | 67 | 15 | 3 | 0 | 0 | 0 |
| $1^--2^+$ | 635 | 614 | 700 | 906 | 1132 | 1288 | 1390 | 1466 |
| $2^+-2^-$ | 705 | 604 | 451 | 252 | 90 | 20 | 3 | 1 |
| $2^--3^+$ | 791 | 716 | 651 | 622 | 693 | 893 | 1121 | 1277 |
| $3^+-3^-$ | 862 | 788 | 712 | 619 | 475 | 271 | 98 | 22 |
| $3^--4^+$ | 927 | 854 | 784 | 715 | 654 | 625 | 693 | 891 |
| $4^+-4^-$ | 986 | 914 | 845 | 777 | 706 | 618 | 475 | 270 |

[a] Potential barriers and vibrational energies are given in $cm^{-1}$.

The double-minimum potential and vibrational levels vary significantly depending on Cl−Cl distances. The barrier heights between double minima are respectively 1161, 2326, 3739, and 5315 $cm^{-1}$ for $R_{ClCl} = 3.50$, 3.60, 3.70, and 3.80 Å. The tunneling splitting of vibrational levels in the double well below the barrier is less than 100 $cm^{-1}$, and the vibrational levels with $v = 0$ for $R_{ClCl} = 3.50$ Å, $v = 0$ and 1 for $R_{ClCl} = 3.60$ Å, $v = 0-2$ for $R_{ClCl} = 3.70$ Å, and $v = 0-3$ for $R_{ClCl} = 3.80$ Å are nearly degenerate.

The 0−1 interval of 1548 or 1605 $cm^{-1}$ for [ClDCl] at $R_{ClCl} = 3.80$ or 3.85 Å, where $R_{ClCl}$ corresponds to the experimental Cl−Cl distance of $3.82 \pm 0.02$ Å in $(DCl)_2$,[12,30] is smaller by about 600 or 500 $cm^{-1}$ than that of 2091 $cm^{-1}$ for DCl, indicating the influence of the hydrogen bonding in [ClDCl]. The 1−2 interval is also obtained as 1390 or 1466 $cm^{-1}$ at $R_{ClCl} = 3.80$ or 3.85 Å. The energy separations for the 0−1 and 1−2 levels are larger than the experimental spacing of about 1500 and 800 $cm^{-1}$ detected in the photodissociation of $(DCl)_2$. These results suggest that the change in atomic configuration of $(DCl)_2$ may be induced by photoexcitation before the terminal D atom is ejected. On the other hand, [ClDCl] with Cl−Cl distances shorter than 3.55 Å gives the 0−1 and 1−2 separations smaller than the oscillating spectrum of the dissociated D atom. Thus, it is expected that the experimental observation may correspond to the vibrations in [ClDCl] with the Cl−Cl distance between 3.60 and 3.75 Å.

## IV. Calculated and Observed Line Spacing of [ClDCl]

In the previous works,[4,5] we studied the 243-nm photodissociation of $(DCl)_2$ selected by the 1-m electrostatic hexapole field followed by the Doppler-selected time-of-flight (DS-TOF) technique. The DS-TOF spectrum of the translational energy distribution for the dissociated D atom is shown in Figure 4a−d. Broken and solid spectra represent the experimental data before and after smoothing, respectively. The six peaks appeared in the experimental spectrum and the first five peak positions were assigned from experimental data as 5010, 3490, 2680, 1890, and 1120 $cm^{-1}$, where the peak at 5010 $cm^{-1}$ corresponds to the vibrational level of $v = 0$. The spacing of adjacent peak positions indicates a significant difference from the fundamental frequency of 2091 $cm^{-1}$ of the stretching mode in DCl. Therefore, the DS-TOF structure suggests a transient vibrational environment of [ClDCl], which is caused by strong perturbation due to the adjacent Cl atom. At this stage, quantitative

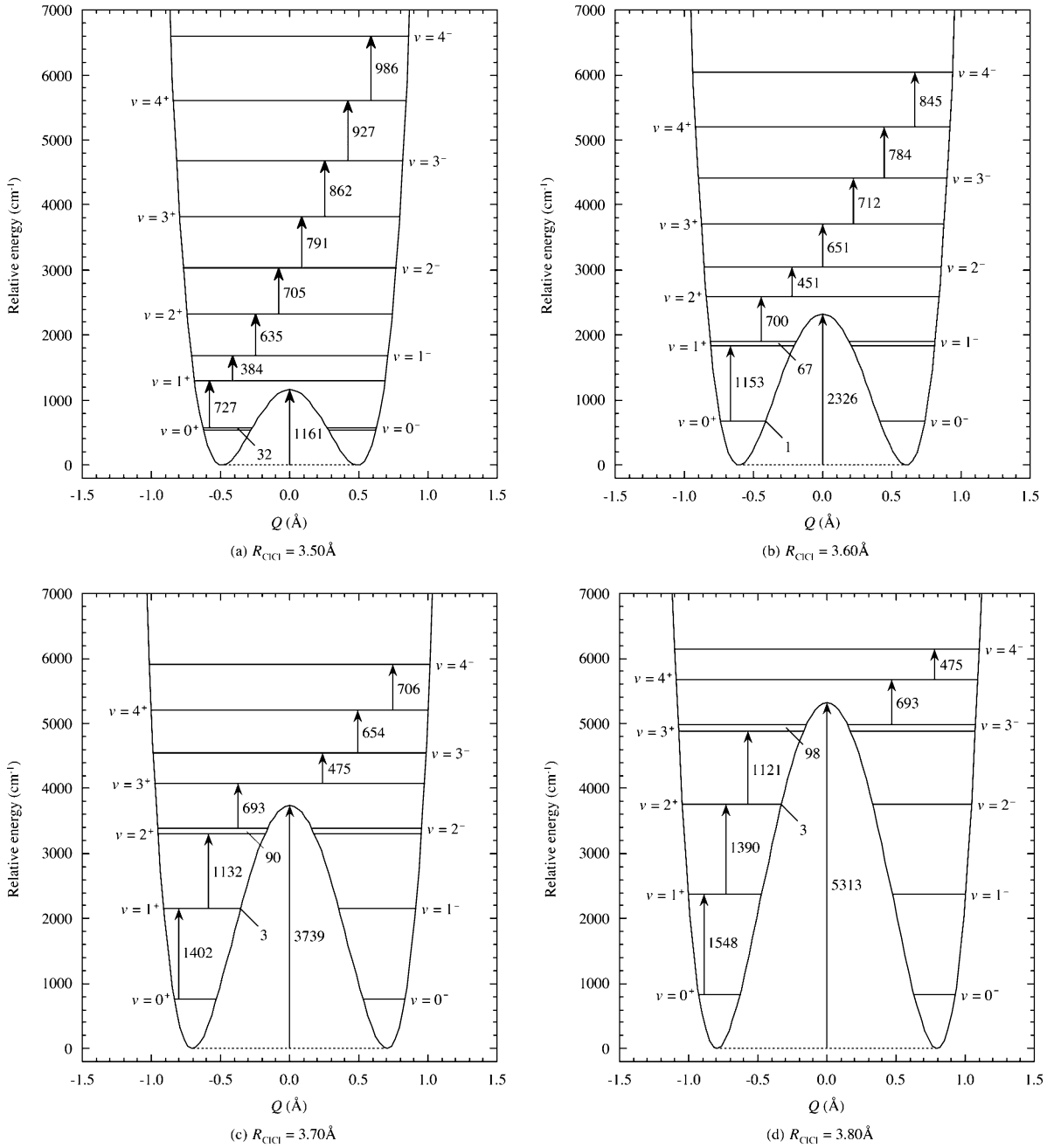


**Figure 3.** Vibrational levels of [ClDCl] with $R_{ClCl}$ = (a) 3.50, (b) 3.60, (c) 3.70, and (d) 3.80 Å.

clarification on the assignment of the nascent vibrational states of [ClDCl] should be necessary to understand the dynamics of $(DCl)_2$ photodissociation as well as the nature of the transition state in the Cl + DCl reaction with the aid of theoretical calculations.

We compare the vibrational spacing between calculation and experiment at $R_{ClCl}$ = 3.60, 3.65, 3.70, and 3.75 Å in Figure 4a−d. The calculated spacing listed in Table 2 is indicated as solid lines above spectrum. The symmetrically combined Morse potential model gives the relative peak positions as follows (the first peak is assigned to the experimental peak at 5010 $cm^{-1}$): 5009, 3856, 3788, 3088, 2637, 1986, 1274, and 490 $cm^{-1}$ for $R_{ClCl}$ = 3.60 Å in Figure 4a; 3709, 3695, 2788, 2537, 1915, 1295, and 580 $cm^{-1}$ for $R_{ClCl}$ = 3.65 Å in Figure 4b; 3608, 3605, 2474, 2384, 1691, 1216, and 563 $cm^{-1}$ for $R_{ClCl}$ = 3.70 Å in Figure 4c; and 3528, 2240, 2220, 1327, 1056, and 432 $cm^{-1}$ for $R_{ClCl}$ = 3.75 Å in Figure 4d. The peak position at 3088 $cm^{-1}$ of [ClDCl] with $R_{ClCl}$ = 3.60 Å obtained from calculation does not correspond to any experimental peaks as shown in Figure 4a. With regard to [ClDCl] with $R_{ClCl}$ = 3.75 Å, the peak positions at 2240, 2220, and 1327 $cm^{-1}$ obtained from calculation do not coincide with any experimental peaks and the third and fourth experimental peaks at 2680 and 1890 $cm^{-1}$ are also not assigned to any calculated peak positions as seen in Figure 4d. On the other hand, it is possible to fairly assign the experimental peaks by the calculated line spacings for [ClDCl] at $R_{ClCl}$ = 3.65 or 3.70 Å as follows: the first peak to $v = 0^+$ and $0^-$ (degenerate), the second peak to $v = 1^+$ and $1^-$ (degenerate), the third peak to $v = 2^+$ and $2^-$, the fourth peak to $v = 3^+$, the fifth peak to $v = 3^-$, and the sixth peak to $v = 4^+$. Judging from the comparison between calculation and experiment mentioned above, it is suggested that [ClDCl] formed by the 243-nm photodissociation of $(DCl)_2$ may have a Cl−Cl distance between 3.65 and 3.70 Å.

Because the Cl−Cl distance is much shorter in [ClHCl] at the transition state than in $(HCl)_2$ at the ground state, the change

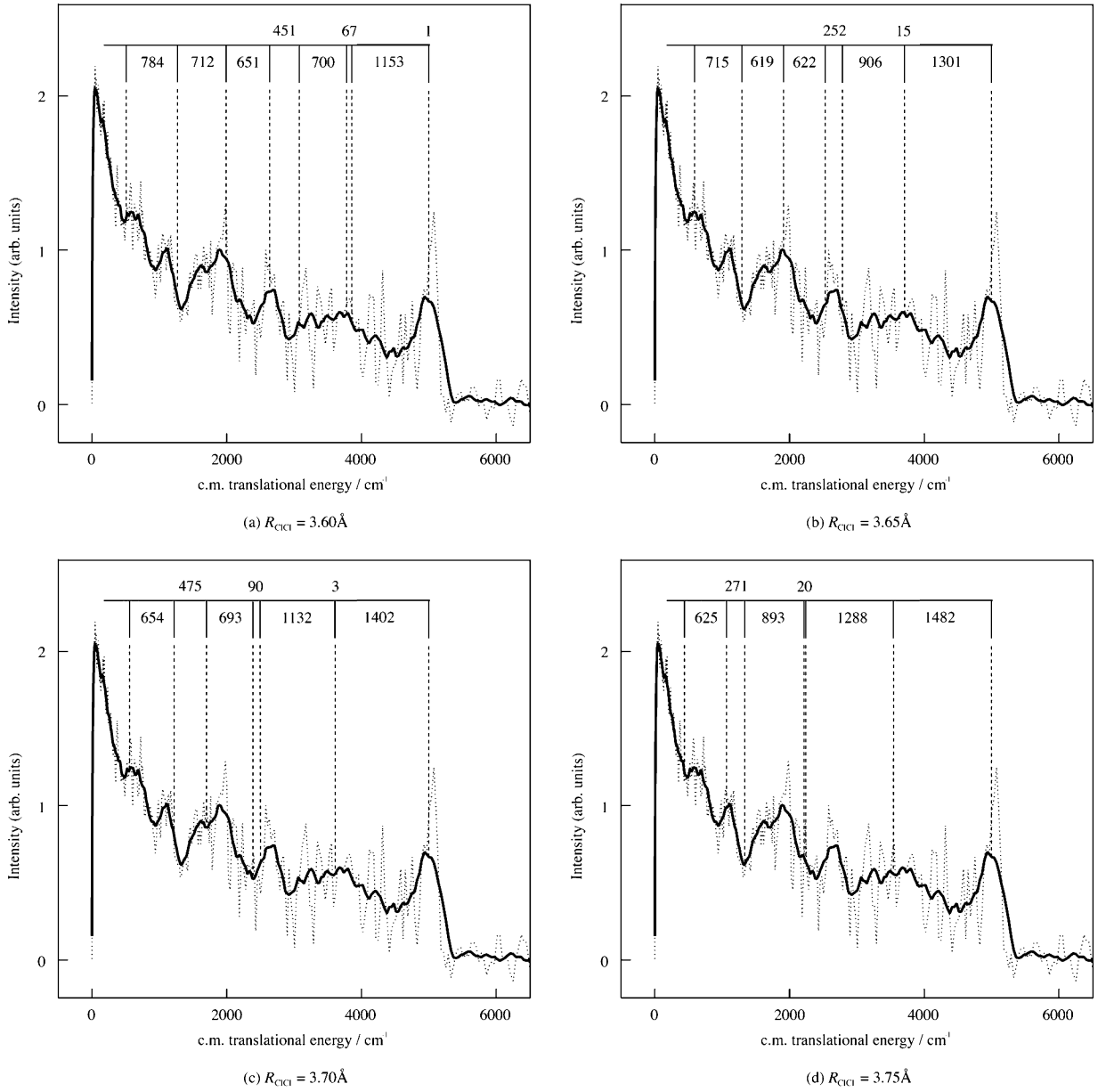


**Figure 4.** Comparison of vibrational spacing between calculation and experiment for $R_{ClCl}$ = (a) 3.60, (b) 3.65, (c) 3.70, and (d) 3.75 Å. The spectra show translational energy distribution of the dissociated D atom reported in refs 4 and 5. Broken and solid spectra represent experimental data before and after smoothing, respectively. Calculated spacing given in Table 2 is indicated as solid lines above the spectra.

in $R_{ClCl}$, which tends to become shorter, may be reasonable if the dissociation of $(DCl)_2$ by eliminating the terminal D atom generates [ClDCl] near the transition state region under one-dimensional dynamics.

## IV. Conclusions

In the present study, we estimate the line spacings of vibrational levels for antisymmetric stretching in linear [ClDCl] by applying the symmetrically combined Morse potential model. The potential energy curve and vibrational levels show significant dependence on the Cl−Cl distance, and the tunneling splitting of vibrational levels below the potential barrier is found to be less than 100 cm$^{-1}$.

The calculated spacings between vibrational levels correspond well to the observed peak spacings for [ClDCl] with Cl−Cl distances of 3.65 or 3.70 Å. Therefore, it is suggested that the oscillating D translational energy distribution detected in the photodissociation of $(DCl)_2$ is caused by the antisymmetric stretching in [ClDCl] with a shorter Cl−Cl distance than $(DCl)_2$.

Finally, the limitation of this work should be noted. Although the correlation between experimental velocity distributions of the ejected D atom and theoretical antisymmetric vibrations of the counterpart [ClDCl] molecule is confirmed in the present study with the one-dimensional model, further work is needed to explain the reaction mechanism in detail since the bond dissociation dynamics occurs in three dimensions.

**Acknowledgment.** This work was done as a research project (research and development of system technologies for resource recycling and minimum energy requirement) financially supported by CREST of JST.

## References and Notes

(1) *Molecular Reaction Dynamics and Chemical Reactivity*; Levine, R. D., Bernstein, R. B., Eds.; Oxford University Press: New York, 1987.

(2) Neumark, D. M. *Acc. Chem. Res.* **1993**, *26*, 33−40.

(3) Metz, R. B.; Weaver, A.; Bradforth, S. E.; Kitsopoulos, T. N.; Neumark, D. M. *J. Phys. Chem.* **1990**, *94*, 1377−1388.

(4) Che, D.-C.; Hashinokuchi, M.; Shimizu, Y.; Ohoyama, H.; Kasai, T. *Phys. Chem. Chem. Phys.* **2001**, *3*, 4979−4983.
(5) Che, D.-C.; Hashinokuchi, M.; Kasai, T.; Kobayashi, D.; Mitani, M.; Yoshioka, Y. *Bull. Pol. Acad. Sci. Chem.* **2002**, *50*, 491−499.
(6) Tao, F.-M.; Klemperer, W. *J. Chem. Phys.* **1995**, *103*, 950−956.
(7) Wesolowski, T. A. *J. Chem. Phys.* **1997**, *106*, 8516−8526.
(8) Garacía, A.; Cruz, E. M.; Sarasola, C.; Ugalde, J. M. *J. Mol. Struct.* (*Theochem*) **1997**, *397*, 191−197.
(9) Latajka, Z.; Scheiner, S. *Chem. Phys.* **1997**, *216*, 37−52.
(10) Meredith, A. W.; Ming, L.; Nordholm, S. *Chem. Phys.* **1997**, *220*, 63−78.
(11) Zhong, Q.; Poth, L.; Ford, J. V.; Castleman, A. W., Jr. *Chem. Phys. Lett.* **1998**, *286*, 305−310.
(12) Burda, J. V.; Hobza, P.; Zahradník, R. *Chem. Phys. Lett.* **1998**, *288*, 20−24.
(13) Silvi, B.; Wieczorek, R.; Latajka, Z.; Alikhani, M. E.; Dkhissi, A.; Bouteiller, Y. *J. Chem. Phys.* **1999**, *111*, 6671−6678.
(14) Halkier, A.; Klopper, W.; Helgaker, T.; Jørgensen, P.; Taylor, P. R. *J. Chem. Phys.* **1999**, *111*, 9157−9167.
(15) Elrod, M. J.; Saykally, R. J. *J. Chem. Phys.* **1995**, *103*, 933−949.
(16) Garrett, B. C.; Truhlar, D. G.; Wagner, A. F.; Dunning, T. H., Jr. *J. Chem. Phys.* **1983**, *78*, 4400−4413.
(17) Vincent, M. A.; Connor, J. N. L.; Gordon, M. S.; Schatz, G. C. *Chem. Phys. Lett.* **1993**, *203*, 415−422.
(18) Visscher, L.; Dyall, K. G. *Chem. Phys. Lett.* **1995**, *239*, 181−185.
(19) Schatz, G. C. *J. Chem. Phys.* **1989**, *90*, 3582−3589.
(20) Gazdy, B.; Bowman, J. M. *J. Chem. Phys.* **1989**, *91*, 4615−4624.
(21) Rougeau, N.; Kubach, C. *Chem. Phys. Lett.* **1994**, *228*, 207−212.
(22) Rougeau, N.; Marcotte, S.; Kubach, C. *J. Chem. Phys.* **1996**, *105*, 8653−8660.
(23) Yamashita, K.; Morokuma, K. *J. Chem. Phys.* **1990**, *93*, 3716−3717.
(24) Yamashita, K.; Morokuma, K. *J. Chem. Phys.* **1991**, *94*, 831.
(25) Mori, K.; Ichimura, A.; Kagawa, H. *J. Mol. Struct.* (*Theochem*) **2002**, *581*, 31−36.
(26) Mitani, M.; Kobayashi, D.; Yoshioka, Y.; Che, D.-C.; Kasai, T. Unpublished results.
(27) Cashion, J. K. *J. Chem. Phys.* **1963**, *39*, 1872−1877.
(28) Huber, K. P.; Herzberg, G. H. *Molecular Spectra and Molecular Structure. Constants of Diatomic Molecules*; Van Nostrand Reinhold: New York, 1979.
(29) Bernath, P. F. *Spectra of Atoms and Molecules*; Oxford University Press: New York, 1995.
(30) Maillard, D.; Schriver, A.; Perchard, J. P.; Girardet, C. *J. Chem. Phys.* **1979**, *71*, 505−516.